

POINT-CONTACT SPECTROSCOPY OF MAGNESIUM DIBORIDE WITH DIFFERENT COUNTER-ELECTRODES

A. I. D'YACHENKO[†], V. YU. TARENKOV[†], M. A. BELOGOLOVSKII[†],
V. N. VARYUKHIN[†], A. V. ABAL'OSHEV^{‡*} AND S. J. LEWANDOWSKI[‡]

[†]*Donetsk Physical and Technical Institute, National Academy of Sciences of Ukraine, R.
Luxemburg 72, 83114 Donetsk, UKRAINE*

[‡]*Instytut Fizyki Polskiej Akademii Nauk, Al. Lotników 32, 02-668 Warszawa, POLAND
abala@ifpan.edu.pl*

Received November 15, 2018

We report on tunneling and Andreev-reflection conductance spectra of 39 K superconducting magnesium diboride, obtained with Pb and Au counter-electrodes. Two distinct steps at close to 2.7 and 7.1 meV appear in a low-resistance metallic-type Au-MgB₂ junction characteristic, whereas a tunneling-like spectrum measured for the same junction, annealed by the application of dc current, exhibits only a rounded contribution of the larger gap. Junctions with a superconducting lead counter-electrode pressed into a bulk MgB₂ sample reveal two conductance peaks that are interpreted as the result of the formation of highly-transmitting break junctions inside the magnesium diboride ceramic. Our results strongly support the two-band model with two different gap values on quasi-two-dimensional σ (7.1 meV) and three-dimensional π (2.7 meV) Fermi surface sheets of MgB₂.

PACS Number(s): 74.25.Kc, 74.45.+c, 74.50.+r, 74.70.Ad

1. Introduction

The discovery of superconductivity in the simple binary compound, MgB₂, generated an intense research activity – mainly, because MgB₂ exhibits a transition temperature T_c of 39 K, which is almost two times higher than that of any other intermetallic superconductor known earlier ¹, but also because of good perspectives for practical applications. During the two years, which have passed from this discovery, our understanding of physical properties of the novel superconductor has made rapid progress.

After confirmation ² of the spin-singlet type of the Cooper pairs involved, the main discussions relating to fundamental physics concentrated on two issues: the mechanism of the Cooper pair formation and the symmetry of the order parameter. The boron isotope effect experiments ³ were the first indication of phonon-

*Corresponding author.

mediated superconductivity. Direct experimental probes of phonon-induced structures in point-contact^{4,5,6,7} and tunneling⁸ superconducting junctions have provided unequivocal support to the theories^{9,10,11,12,13,14}, which explain the relatively high T_c as originating from the strong anharmonic electron-phonon coupling to Raman-active high-frequency E_{2g} vibration modes, corresponding to the in-plane distortions of the boron hexagons.

It took much longer to elucidate the properties of the superconducting order parameter, but now from the results of tunneling and photoemission spectroscopy, specific heat, and other measurements emerged strong experimental evidence that magnesium diboride belongs to a rare class of materials with two gaps of different widths, which arise from a huge anisotropy of electronic properties (*cf* the review of tunneling data for magnesium diboride¹⁵). The Fermi surface of MgB_2 is very anisotropic and consists of four bands: two σ -type quasi-two-dimensional cylindrical hole sheets and two π -type three-dimensional tubular networks, exhibiting very different electron-phonon coupling strengths¹⁶. As a result, the superconducting gap varies considerably on the Fermi surface and, as follows from first-principles' calculations¹⁴, clusters into two groups. The σ cylindrical sheets relate to a larger gap of an average value of 7 meV with small variations, while the smaller gap ranges from 1.2 to 3.7 meV on the three-dimensional π sheets. These calculations support a two-gap scenario for magnesium diboride, originally proposed by Shulga *et al.*¹⁷ in order to explain the behavior of the upper critical magnetic field. It should be noted that, in contrast to conventional superconductors, impurity scattering does not average out strongly different gap values. Averaging becomes ineffective in MgB_2 because the different symmetry of σ - and π -type bands makes interband scattering much weaker than intraband impurity mixing of electron states¹⁸.

Based on such ideas, an effective two-band model with $\Delta_\sigma(T=0) = 7.1$ meV and $\Delta_\pi(T=0) = 2.7$ meV was derived, and consequences for tunneling into MgB_2 were deduced¹⁹. The discussion of our tunneling and point contact data relating to the energy gap distribution will be mainly based on this model and will use a minimal number of fitting parameters. Most samples studied previously were in the intermediate regime between a direct metallic contact and a tunnel junction with a strong insulating (I) barrier. The main conclusions for these structures have been drawn by fitting the differential conductance data to the one-dimensional Blonder-Tinkham-Klapwijk (BTK) model²⁰, modified by introducing a damping parameter Γ , and by taking into account two possible channels for the charge transport, so that not only the gap values, but also the ratio of the individual channel contributions were taken as adjustable parameters. In this paper, we present the data for low-resistance junctions with a gold counter-electrode, which to our knowledge are the first reported direct metallic-type contacts with superconducting MgB_2 , and which can be described within the two-band model¹⁹ without any additional parameters. Moreover, by applying dc current pulses we have successfully transformed the clean contact into a high-resistance tunneling junction, and reproduced in this way the two limiting regimes of the theory¹⁹. The second issue, which is discussed in the

paper, is the assertion by Schmidt *et al.*^{15,21} that pressing a counter-electrode into the MgB₂ sample often breaks off an MgB₂ crystal fragment and results (even if we are dealing with a normal (N) injector) in a junction between two (identical) superconductors, instead of the expected normal metal - superconductor structure. Such internal break-junctions apparently can be formed also when a superconducting counter-electrode is pressed into MgB₂. Our experiments with a lead injector provide an independent confirmation of the observation made by Schmidt *et al.*, and fit into the double-gap scenario as well.

2. Results and Discussion

2.1. Sample preparation

We used polycrystalline MgB₂ samples in the form of $15 \times 1 \times 0.1$ mm³ rectangular bars of high density, prepared by compacting commercial magnesium diboride powder at $\sim 20 - 30$ kbar. Magnetization measurements have shown a superconducting transition with the onset and midpoint at 39.0 and 36.5 K, respectively. All experiments were performed at 4.2 K. The junctions based on these samples exhibited mostly no 'native' barrier, and their resistance varied from several to a few tens of Ohms. In order to establish a suitable barrier between the electrodes, we applied short current pulses with an amplitude of several tens of milliamperes and a duration of a few seconds; as a result we obtained junction resistances up to a few hundred Ohms. Two different counter-electrodes have been used: lead and gold. Current I versus voltage V characteristics as well as differential conductance spectra $G(V) = dI(V)/dV$ were measured by conventional four-probe lock-in technique²². In the paper we present typical data obtained in this manner.

The junctions with Pb injector were fabricated by mounting a Pb hemisphere of 0.5 mm diameter on an elastic beryllium strip, which was driven into the MgB₂ surface. Point-contact junctions with an Au counter-electrode were prepared by touching the superconducting surface with a 0.02 mm gold wire wrapped around the MgB₂ sample; the formation of SNS junctions was avoided in this manner. The device was stabilized by a coat of varnish. This procedure, which yielded junction resistance of about 10Ω and conductance spectra indicating a direct heterostructure formed by normal and superconducting electrodes, could in principle produce several point contacts instead of a single one. Such occurrence is not important in the case of clean junctions, since in such a case the spectral contribution of the contacts with transparency significantly smaller than unity is negligible. In our best Au-MgB₂ samples, an almost ideal metallic Sharvin contact between gold and magnesium diboride was formed. This can be seen from the conductance drop with voltage increase from $V = 0$ to Δ_σ/e (figure 2). The drop is almost by a factor of two, with the small deviation attributed to damping and thermal smearing effects.

2.2. *Pb-MgB₂ junctions*

The junctions with a Pb injector were prepared in an analogous manner to that used by Schmidt *et al.*²¹, who formed symmetric MgB₂ – MgB₂ structures by breaking off an MgB₂ crystal fragment under the tip pressure. Following the arguments of the cited work, we also suppose that our Pb-MgB₂ samples are symmetric break junctions inside the magnesium diboride bulk, rather than contacts between two different superconductors. The nature of the junction barrier is unknown, but its small resistance compared to that of the SIS structures²¹ suggests that we are dealing rather with SNS contacts (see also the paper of Gonnelli *et al.*²³ and arguments given below). The initial $I(V)$ characteristic exhibited a critical supercurrent at zero bias $I_c \sim 0.9$ mA and normal-state resistance $R_N = 1.8 \Omega$, i.e., $I_c R_N \sim 1.6$ mV [plot 1 in the inset in figure 1(a)]. This value of $I_c R_N$ is significantly lower than that predicted by the model¹⁹ for a Josephson current across a symmetric MgB₂ – MgB₂ device, but is consistent with $I_c R_N$ values found previously by two other groups^{23,21} for break junctions of magnesium diboride.

The evolution of the interface properties of the junctions, caused by the application of the forming current pulses, is clearly visible in the current-voltage characteristics shown by the inset in figure 1(a). After two successive current pulses (characteristics ‘2’ and ‘3’ in the inset), we obtained a finite resistance $R_N = 3.6 \Omega$ at zero bias (characteristic ‘3’). The latter characteristic, shown in the main panel of figure 1(a) in a larger voltage scale, exhibits an excess current I_{exc} known to be the manifestation of Andreev reflections in high-transparency superconducting heterostructures. Remarkably, only twofold increase of junction resistance was sufficient to suppress the supercurrent, whereas the Josephson current in reference²¹ was visible up to contact resistances of about 10 k Ω . Our result can indicate that we create multiple incoherent-scattering centers and the Josephson current is cancelled because of the phase-breaking events. Liao *et al.*²⁴ found that magnesium diboride samples prepared by solid-state reaction contain large amounts of precipitates composed mainly of magnesium and oxygen. We believe that their presence is the origin of a strong damping factor in conductance spectra of MgB₂ (even without any current treatment), stressed in almost all publications on point-contact spectroscopy of this compound. It is highly probable that by applying current pulses, we create such centers and destroy the phase coherence during the charge transfer across the interface region between two superconducting banks.

To further verify the hypothesis of the SNS symmetric break-junctions formed inside MgB₂ bulk, let us analyze the high-voltage asymptote of the current-voltage characteristic shown in figure 1(a) and known to be determined by a set of inter-layer transparencies²⁷. Their distribution has been found in two extreme cases: for a diffusive normal conductor by Dorokhov²⁵ and for a disordered insulating interface by Schep and Bauer²⁶ (see also Naveh *et al.*²⁷). For two identical superconductors both theories predict $I(V) = G_N(V + k\Delta/e)$, where the last term is the excess current I_{exc} . For the Dorokhov distribution, the coefficient $k = 1.467$, while

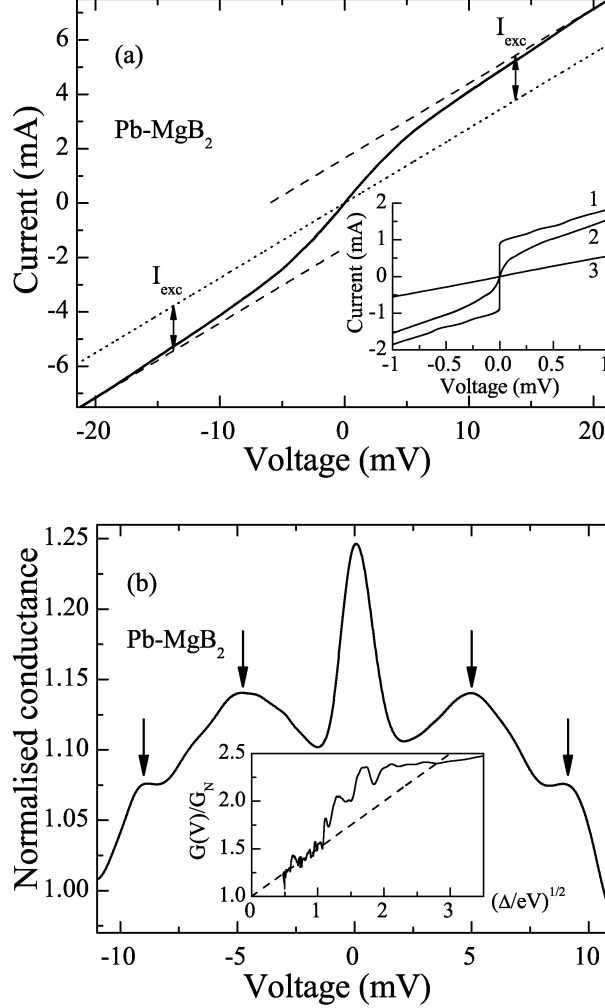


Fig. 1. Current and differential conductance in function of voltage for a junction formed by pressing Pb into MgB₂ bulk sample: (a) $I - V$ characteristic at $T = 4.2$ K of a current modified junction (marked 3 in the inset) exhibiting an excess current $I_{\text{exc}} = 1.6$ mA (solid line in the main panel); the dotted line was measured in the normal state. The inset shows successive modifications of the $I - V$ characteristics (labelled 1 to 3) after applying short current pulses. (b) differential conductance normalized to the conductance at 20 mV corresponding to characteristic 3 demonstrates a prominent zero-bias maximum with two peaks on each side (arrows indicate voltage positions of the combinations of small and large gap values $2\Delta_{\pi}/e$ and $\Delta_{\sigma}/e + \Delta_{\pi}/e$). The inset shows $G(V)/G_N$ corresponding to characteristic 2 as a function of $\sqrt{\Delta/eV}$ (continuous line) and the plot of the theoretical²⁸ interpolating formula for disordered SNS junctions $G(V)/G_N = 1 + 0.5\sqrt{\Delta/eV}$ (dashed line); the best fit was found for $\Delta = 6.8$ meV.

within the Schep-Bauer approximation, $k = 1.055$ ²⁷. Applying the arguments of reference²⁰, we presume that for dissimilar superconductors with gap values Δ and

Δ' the excess current in a SNS' junction is given by $I_{\text{exc}}R_N \approx k(\Delta + \Delta')/(2e)$. We can perform then an analysis similar to that presented in reference ¹⁹ for the dc Josephson current. For a symmetric $\text{MgB}_2 - \text{MgB}_2$ structure we conclude that the $I_{\text{exc}}R_N$ product should vary from $\lesssim 4$ mV (tunneling along the c -axis direction) to 6 mV (tunneling within the $a - b$ plane) in the case of a S-diffusive N-S structure, and between 3 mV to 5 mV in the case of a disordered insulating interface. At the same time, for a contact formed by a conventional superconductor like Pb with a single gap equal to 1.4 mV, the $I_{\text{exc}}R_N$ value cannot exceed 4 mV in any model. From figure 1(a) we find $I_{\text{exc}}R_N = 5.7$ mV, i.e. a value much greater than the latter limit. This strongly supports the thesis that the weak link in our structures with lead counter-electrode is not at the interface of the contacting materials but rather inside the magnesium diboride bulk. Furthermore, the product $I_{\text{exc}}R_N$ exceeds the upper limit for the Schep-Bauer distribution, providing an argument for the SNS nature of the junction.

To verify further this scenario, let us compare our dc differential conductance with the predictions of the scattering-matrix theory of multiple Andreev reflections in short disordered SNS junctions ²⁸. Using zero voltage asymptotic behavior of the dc differential conductance $G(V) = dI(V)/dV$ (equation (14) of reference ²⁸), we can check on the background behavior of our conductance spectra. We apply an interpolating formula $G(V) = G_N(1 + 0.5 \tanh(\Delta/2T)\sqrt{\Delta/eV})$, which is valid both at very low bias (the near-zero-bias $1/\sqrt{V}$ singularity is the hallmark of Andreev-reflection processes occurring at each junction face), and at very high voltages (in the latter case $G(V)$ is equal to the normal-state value $G_N = 1/R_N$). Using Δ as a fitting parameter, we found that the best agreement with the experimental data is achieved for $\Delta = 6.8$ meV. The overall behavior of the experimental normalized conductance $G(V)/G_N$ corresponding to the experimental data and plotted in function of $\sqrt{6.8/eV}$ is satisfactorily described [see the inset in figure 1(a)] by a simple fitting line $G(V)/G_N = 1 + 0.5\sqrt{\Delta/eV}$ in the voltage range above 0.5 mV, where temperature smearing is not effective. In the small bias region up to 15 meV, the conductance exhibits a fine structure, which according to Bardas and Averin ²⁸ can be attributed to subharmonic gap singularities, as well as to the gap features.

Characteristic '3' is more smooth than '2', and the corresponding differential conductance presented in the main panel of figure 1(b) contains a strongly suppressed zero-bias peak and two maxima. Their voltage positions are very close to the combinations of small and large gap values $2\Delta_\sigma/e$ and $\Delta_\sigma/e + \Delta_\pi/e$ expected for the magnesium diboride ¹⁹ and shown in figure 1(b) by arrows. We should emphasize that we do not observe any signs of the lead gap. Moreover, the features discussed above, including the peak at $V = 0$, are seen at temperatures exceeding the T_c of Pb, and this rules out their possible relation to the lead counter-electrode.

2.3. *Au-MgB₂ point contact junctions*

Let us examine now the conductance spectra of our Au-MgB₂ point contacts in the framework of a double-gap model with fixed gap values and weighing factors¹⁹. These quantities are found from first-principles' calculations, therefore the adjustable parameters are reduced to the barrier strength and the damping factor Γ . The latter one was introduced into the tunneling density of states by Dynes *et al.*²⁹ and is often referred to as the Dynes factor. The barrier strength is measured by a parameter $Z = \int_0^d H(x) dx / \hbar v_F$ ²⁰, where $H(x)$ is the barrier height, x denotes the coordinate normal to the interface, d is the barrier width, and v_F is the x -component of the Fermi velocity. The conductance spectrum $G(V)$ is assumed to be a sum of two single-mode BTK contributions²⁰ related to the two σ - and π -type bands in proportions strongly depending on the injection angle. The relevant weighting factors, which determine the ratio of the two contributions, are proportional to the squared plasma frequencies and are given in reference¹⁹ for the transport within the $a-b$ plane, $G_{a-b}(V)$, and for tunneling in the c -axis direction, $G_c(V)$. In the present experiment, the conductance is a mixture of $a-b$ plane and c -axis contributions with unknown coefficients, which can be different for different polycrystalline samples. Only to get a qualitative estimate of the averaged conductance spectra predicted by the theory, we compare the measured spectra with the mean characteristic $G_m(V) = [G_{a-b}(V) + G_c(V)]/2$. As it was stated above, we prefer to obtain qualitative conclusions with a limited number of fitting parameters rather than to introduce weighting factors with the aim to improve the agreement between theory and experiment.

In reference¹⁹, a two-step structure was predicted for a direct contact between a normal-metal injector and magnesium diboride and for charge transport in the $a-b$ plane (upper curve in the inset in figure 2 calculated for $T = 0$). For the c -axis transport, the main contribution comes from the π band (curve 2 in the inset). The averaged characteristic (see curve 3 in the inset and the dashed curve in the main panel), which takes into account a small Dynes factor Γ and temperature smearing effects determined by a standard procedure involving Fermi distribution functions, qualitatively well reproduces the two-step feature observed by us experimentally (solid line in figure 2). It should be stressed that this good agreement of experiment and theory was obtained with a single fitting parameter Γ .

We formed next a low-transparency insulating (I) barrier in our Au-I-MgB₂ junctions by applying additional current pulses and measured the resultant $G(V)$ characteristics in a wide range of bias voltages (up to 100 meV). The conductance background usually exhibited a roughly parabolic dependence on voltage, with a very small offset of minimum from $V = 0$ (see figure 3), indicating an almost symmetrical barrier²² and proving the tunneling character of the charge transport. A simple formula³⁰ for a rectangular potential barrier may be used to find an average barrier height H and its thickness d . In order to carry out the evaluation, we need

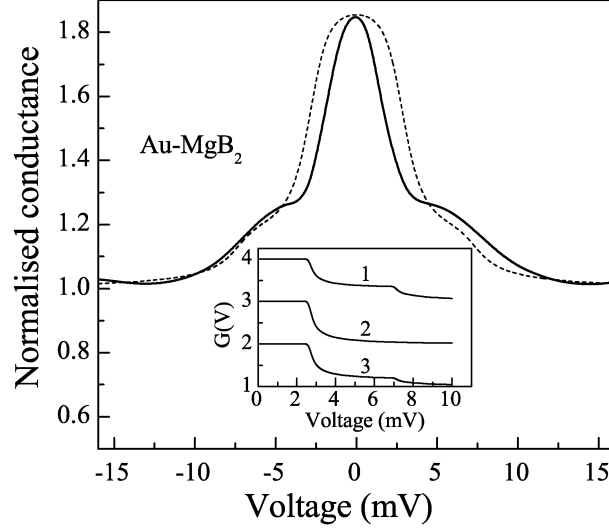


Fig. 2. Conductance spectrum at $T = 4.2$ K of a direct Au-MgB₂ contact ($R_N = 20.5 \Omega$), normalized to the conductance at 20 mV (solid line). The dashed line represents a mean characteristic $G_m(V)$ calculated from the two-gap model¹⁹ in the limit of a completely transparent interface and $Z = 0$, small smearing parameter $\Gamma = 0.23$ and $T = 4.2$ K. The inset shows zero-temperature theoretical plots of conductance ($Z = 0$, $\Gamma = 0$): 1 – charge transport within the ab -plane, 2 – transport along the c -axis, 3 – mean conductance $G_m(V)$; the plots are displaced vertically for clarity.

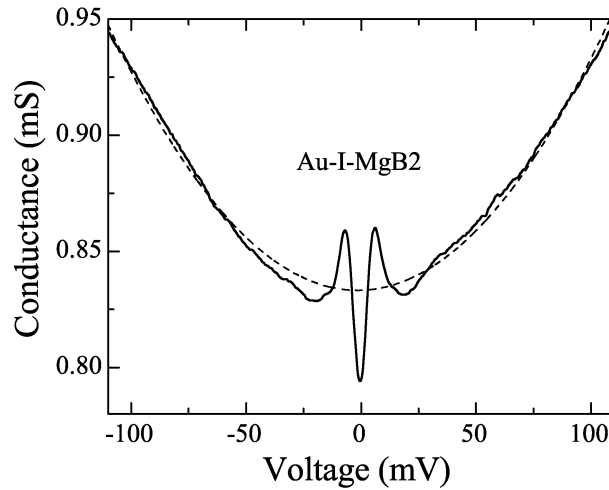


Fig. 3. Conductance at $T = 4.2$ K of a tunneling Au-I-MgB₂ junction with normal-state resistance $R_N = 1.2 \text{ k}\Omega$ formed by applying several current pulses (solid line). The dashed line shows a parabolic fit.

the contact area, which is unknown. Nevertheless, a minimal value for Z parameter can be estimated from the parabolic shape of the conductance curve. According to reference ³⁰, the coefficient κ in the quadratic term in the voltage dependence of conductance, $G(V)/G(0) = 1 + (eV/\kappa)^2$, is given by $\kappa = H^{1/2}/(0.182d)$, where H is in volts and d is in Ångströms. We assume d to be not less than two-three lattice parameters and take as a minimum $d = 10$ Å. Substituting κ found from the measured conductance background (figure 3), we obtain $Z > 0.85$. Consequently, we take the first fitting parameter Z equal to 0.9.

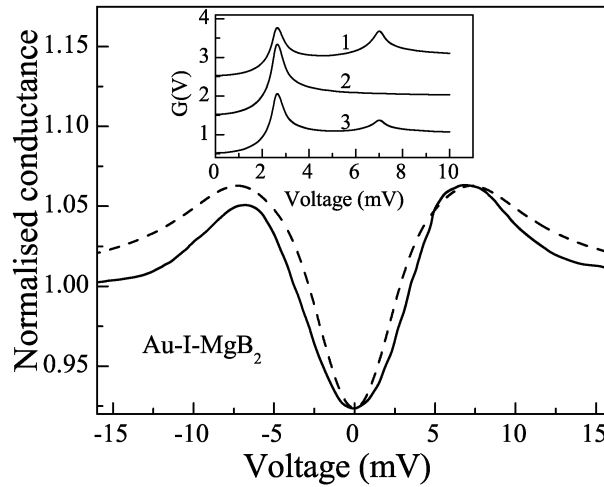


Fig. 4. Tunneling-like conductance spectrum of Au-I-MgB₂ junction with normal-state resistance $R_N = 1.2$ k Ω normalized to the conductance at 20 mV (solid line). The dashed line represents the calculated mean characteristic $G_m(V)$ following the two-gap model ¹⁹ for $Z = 0.9$, $\Gamma = 2.9$, $T = 4.2$ K. The inset shows zero-temperature theoretical curves for $Z = 0.9$ and vanishing damping parameter Γ : 1 – charge transport within the ab -plane, 2 – transport along the c -axis, 3 – mean characteristic $G_m(V)$. The plots in the inset are displaced vertically for clarity.

In figure 4, the main panel presents the measured conductance spectrum of the same junction in the near-gap voltage region, while in the inset we show the conductance calculated for tunneling into the $a-b$ plane and along the c -axis direction for vanishing Dynes factor, $\Gamma = 0$. The latter characteristics clearly indicate that the most pronounced feature in the average conductance spectrum should be the smaller gap peak, whose signature is missing from the measured spectrum. The most probable cause is the strong disorder induced by the forming current pulses and the resulting significant inelastic scattering near the interface. For large values of Γ (the second fitting parameter) the agreement between the experimental and calculated conductances is very good, as shown in the main panel in figure 4.

To conclude the discussion of near-gap features in the junction characteristics, let us make two remarks concerning the role of disordering effects. The analysis

based on a simple BTK approach²⁰ for describing the experiment with (probably) numerous elastic and inelastic scatterers randomly distributed within the barrier appears to be somewhat naive, nevertheless is justified, since one can always introduce an effective transparency parameter Z within a single-mode model²⁰ by integrating over a certain distribution of transparencies (see the corresponding discussion in reference²⁸). It should be stressed that the additional averaging already takes into account the possible appearance of multiple point contacts in our experiments. The averaging provides some additional smearing, but the most transparent contacts will dominate in the spectrum.

The second remark concerns the possibility of observing double-gap spectrum in a disordered superconductor with important charge scattering. Our samples contain comparatively large grains. Therefore, we expect that the measured characteristics of a clean point contact reflect the bulk properties of the material. It is known that dense bulk samples of MgB₂ are usually in the clean limit, with the elastic mean free path large in comparison to the superconducting coherence length. This condition is necessary to observe two distinct gaps in a sufficiently clean superconductor. At the same time, our method of fabricating the insulating layer between the electrodes generates, as it was argued above, a great amount of inelastic-scattering inclusions. At first sight, the interband impurity scattering should cause the gaps to converge. But this is not the case for magnesium diboride. According to reference³¹, optical properties of dense polycrystalline samples of MgB₂, as well as a surprisingly small correlation between the defect concentration and T_c , can be understood only by assuming negligibly small inter-band impurity scattering. The possible reason is in the specific electronic structure of MgB₂, namely the two-dimensional σ -band states overlap slightly with the states in the Mg plane, where defects are most likely to occur¹⁸. Thus one can expect that the interband scattering rate between the σ - and π -bands is small, even in low-quality samples.

3. Conclusions

In summary, we have realized several different types of heterostructures based on superconducting magnesium diboride: from a low-resistance (almost ideal) Au-MgB₂ point contact to an SNS junction (with a lead counter-electrode) obtained by applying current pulses. Moreover, with this technique we have succeeded to transform point-contact samples with gold injector into tunnel-like devices. In the case of lead electrode, we have confirmed the observation of Schmidt *et al.*¹⁵ that pressing the electrode can result in the formation of symmetric superconductor-superconductor junctions inside the magnesium diboride bulk. Our findings for Au and Pb counter-electrodes were interpreted within the two-gap model for the energy spectrum of MgB₂ and thus provide novel arguments in favor of a multi-band scenario for magnesium diboride.

Acknowledgements

This work was partially supported by the Polish Committee for Scientific Research (KBN) under Grant No. PBZ-KBN-013/T08/19 and by INTAS under project No. 2001-0617.

References

1. C. Buzea and T. Yamashita, *Supercond. Sci. Technol.* **14**, R115 (2001).
2. H. Kotegawa, K. Ishida, Y. Kitaoka, T. Muranaka and J. Akimitsu, *Phys. Rev. Lett.* **87**, 127001 (2001).
3. S. L. Bud'ko, G. Lapertot, C. Petrovic, C. E. Cunningham, N. Anderson and P. C. Canfield, *Phys. Rev. Lett.* **86**, 1877 (2001).
4. N. L. Bobrov, P. N. Chubov, Yu. G. Naidyuk, L. V. Tyutrina, I. K. Yanson, W. N. Kang, H.-J. Kim, E.-M. Choi, S. I. Lee, in *New Trends in Superconductivity*, ed. J. F. Annett and S. Kruchinin (Kluwer Academic Publishers, Dodrecht, 2002), vol. **67** , p. 225.
5. Yu. G. Naidyuk, I. K. Yanson, O. E. Kvitnitskaya, S. Lee, S. Tajima, cond-mat/0211134 (2002).
6. I. K. Yanson, V. V. Fisun, N. L. Bobrov, Yu. G. Naidyuk, W. N. Kang, E.-M. Choi, H.-J. Kim, S.-I. Lee, cond-mat/0206170 (2002); I. K. Yanson, Yu. G. Naidyuk, O. E. Kvitnitskaya, V. V. Fisun, N. L. Bobrov, P. N. Chubov, V. V. Ryabovol, G. Behr, W. N. Kang, E.-M. Choi, H.-J. Kim, S.-I. Lee, T. Aizawa, S. Otani and S.-L. Drechsler, cond-mat/0212599 (2002).
7. P. Samuely, P. Szabo, J. Kacmarcik, T. Klein, A. G. M. Jansen, cond-mat/0211544 (2002).
8. A. I. D'yachenko, V. Yu. Tarenkov, A. V. Abal'oshev, S. J. Lewandowski, cond-mat/0201200 (2002).
9. J. M. An and W. E. Pickett, *Phys. Rev. Lett.* **86**, 4366 (2001).
10. Y. Kong, O. V. Dolgov, O. Jepsen and O. K. Andersen, *Phys. Rev.* **B64**, 020501(R) (2001).
11. K.-P. Bohnen, R. Heid and B. Renker, *Phys. Rev. Lett.* **86**, 5771 (2001).
12. A. Y. Liu, I. I. Mazin and J. Kortus, *Phys. Rev. Lett.* **87**, 087005 (2001).
13. H. J. Choi, D. Roundy, H. Sun, M. L. Cohen and S. G. Louie, *Phys. Rev.* **B66** 020513(R) (2002).
14. H. J. Choi, D. Roundy, H. Sun, M. L. Cohen and S. G. Louie, *Nature* **418**, 758 (2002).
15. H. Schmidt, J. F. Zasadzinski, K. E. Gray and D. G. Hinks, *Physica* **C385**, 221 (2003).
16. J. Kortus, I. I. Mazin, K. D. Belashchenko, V. P. Antropov and L. L. Boyer, *Phys. Rev. Lett.* **86**, 4656 (2001).
17. S. V. Shulga, S.-L. Drechsler, H. Eschrig, H. Rosner, W. E. Pickett, cond-mat/0103154 (2001).
18. I. I. Mazin, O. K. Andersen, O. Jepsen, O. V. Dolgov, J. Kortus, A. A. Golubov, A. B. Kuz'menko, D. Van der Marel, *Phys. Rev. Lett.* **89**, 107002 (2002).
19. A. Brinkman, A. A. Golubov, H. Rogalla, O. V. Dolgov, J. Kortus, Y. Kong, O. Jepsen, O. K. Andersen, *Phys. Rev.* **B65**, 180517(R) (2002).
20. G. E. Blonder, M. Tinkham and T. M. Klapwijk, *Phys. Rev.* **B25**, 4515 (1982).
21. H. Schmidt, J. F. Zasadzinski, K. E. Gray and D. Hinks, *Phys. Rev. Lett.* **88**, 127002 (2002).
22. E. L. Wolf, *Principles of Electron Tunneling Spectroscopy* (Oxford University Press, New York, 1985).

12 *A. I. D'yachenko et al.*

23. R. S. Gonnelli, A. Calzolari, D. Daghero, G. A. Ummarino, V. A. Stepanov, G. Giunchi, S. Cerasara and G. Ripamonti, *Phys. Rev. Lett.* **87**, 097001 (2001).
24. X. Z. Liao, A. Serquis, Y. T. Zhu, J. Y. Huang, L. Civale, D. E. Peterson, F. M. Mueller and H. F. Xu, cond-mat/0212571 (2002).
25. O. N. Dorokhov, *Pis'ma Zh. Eksp. Teor. Fiz.* **36**, 259 (1982) [*JETP Lett.* **36**, 318 (1982)]; O. N. Dorokhov, *Solid State Commun.* **51**, 381 (1984).
26. K. N. Schep and G. E. W. Bauer, *Phys. Rev. Lett.* **78**, 3015 (1997); K. N. Schep and G. E. W. Bauer, *Phys. Rev.* **B56**, 15860 (1997).
27. Y. Naveh, V. Patel, D. V. Averin, K. K. Likharev and J. E. Lukens, *Phys. Rev. Lett.* **85**, 5404 (2000).
28. A. Bardas and D. V. Averin, *Phys. Rev.* **B56**, R8518 (1997).
29. R. C. Dynes, V. Narayanamurti and J. P. Garno, *Phys. Rev. Lett.* **41**, 1509 (1978).
30. J. G. Simmons, *J. Appl. Phys.* **34**, 238 (1963).
31. A. B. Kuz'menko, F. P. Mena, H. J. A. Molegraaf, D. Van der Marel, B. Gorshunov, M. Dressel, I. I. Mazin, J. Kortus, O. V. Dolgov, T. Muranaka and J. Akimitsu, *Solid State Commun.* **121**, 479 (2002).